NOTE

Verification of lung dose in an anthropomorphic phantom calculated by the collapsed cone convolution method

Martin J Butson†‡, Rebecca Elferink†, Tsang Cheung‡, Peter K N Yu‡, Michael Stokes‡, Kim You Quach† and Peter Metcalfe†

† Illawarra Cancer Care Centre, Department of Medical Physics, Crown St, Wollongong, NSW 2500, Australia
‡ City University of Hong Kong, Department of Physics and Materials Science, Kowloon Tong, Hong Kong

E-mail: mbutson@usa.net

Abstract. Verification of calculated lung dose in an anthropomorphic phantom is performed using two dosimetry media. Dosimetry is complicated by factors such as variations in density at slice interfaces and appropriate position on CT scanning slice to accommodate these factors. Dose in lung for a 6 MV and 10 MV anterior–posterior field was calculated with a collapsed cone convolution method using an ADAC Pinnacle, 3D planning system. Up to 5% variations between doses calculated at the centre and near the edge of the 2 cm phantom slice positioned at the beam central axis were seen, due to the composition of each phantom slice. Validation of dose was performed with LiF thermoluminescent dosimeters (TLDs) and X-Omat V radiographic film. Both dosimetry media produced dose results which agreed closely with calculated results nearest their physical positioning in the phantom. The collapsed cone convolution method accurately calculates dose within inhomogeneous lung regions at 6 MV and 10 MV x-ray energy.

1. Introduction

A 3D treatment planning system using collapsed cone convolution should provide accurate dosimetry in regions of heterogeneity such as lung (Ahnesjo 1989). In short, the convolution describes radiation interactions including charged particle transport, and calculates dose derived from CT density and patient set up information. Previous tests verifying convolution accuracy have been undertaken in slab lung phantoms with the results showing good agreement in regions of disequilibrium in lung (Mackie *et al* 1985a, Boyer and Mok 1986, Metcalfe *et al* 1993), with only a small overestimation in dose due to rectilinear scaling approximations at high photon energies (Keall and Hoban 1996). The final step in commissioning an RT planning system is verification of the accuracy in an anthropomorphic phantom. This ensures inhomogeneity corrections are performed accurately when phantom geometry and construction closely resembles a real patient. Hence tests were undertaken using thermoluminescent dosimetry and radiographic film techniques. Acceptable quality assurance procedures and associated errors related to treatment planning computers have been previously outlined by Van Dyk *et al* (1993) and Fraass *et al* (1998). Previous dosimetry by Ramsey *et al* (1999) gave results for Pinnacle with lung inhomogeneity using a TG 23 test package, but only to points outside the lung region. Howlett *et al* (1999) performed point verification for a male ART phantom, but outside the lung region using an ionization chamber compared with

collapsed cone convolution. This note examines dose within the lung region of a heterogeneous anthropomorphic phantom.

2. Materials and methods

Calculations were performed on an ADAC† Pinnacle version 5.0e treatment planning system which uses a collapsed cone convolution method for dose calculation. Collapsed cone convolution evolved from convolution/superposition methods developed by Mackie *et al* (1985b), Boyer and Mok (1985) and Mohan *et al* (1986), where the generated TERMA distributions are calculated and then convolved with either analytical or Monte Carlo generated kernels which account for scattered photons and transport of charged particles (Mackie *et al* 1988, Papanikolaou *et al* 1993). The weighting of the TERMA array to account for the polyenergetic nature of the beam is discussed elsewhere (Hoban 1995), as is correction for kernel tilting with beam divergence (Papanikolaou *et al* 1993). The collapsed cone convolution method uses an analytical kernel represented by a set of cones, the energy deposited in which is collapsed onto a line (hence the name). The method is used to reduce computation time. In practice, the method utilizes a lattice of rays, such that each voxel is crossed by one ray corresponding to each cone axis. TERMA is calculated at regular points along each ray and the resulting energy directed into the associated cone is used to increment the dose deposited at points along the ray (via the kernel parameters for that ray angle). Dose at a point is the sum of contributions from each such ray (one for each cone angle), where dose due to each ray is an accumulation of the effect of TERMA at all points on the ray. The polyenergetic spectrum is accounted for in the TERMA calculation via an effective attenuation coefficient, and there is an empirical correction to account for the fact that the kernel parameters do not vary as the primary beam hardens with depth (Papanikolaou *et al* 1993). Adaptive and full collapsed cone options exist. The adaptive variant uses a dose gradient difference method to reduce the time of calculation. No differences in results were observed using either the full or adaptive method.

A modelled 6 MV x-ray beam was used which calculated depth dose results within 2% of measured dose for depths up to 30 cm in water. The calculation grid resolution size used was 4 mm. To examine the affect of grid resolution, tests were performed with resolutions ranging from 2 mm up to 1 cm in size. However, less than 2% variation in applied dose at depth was calculated for these changes in grid resolution, with the beam calculated as slightly more penetrating with smaller grid resolution. The phantom densities used by Pinnacle were calculated from a translation table created using a CT phantom and the values were reproducible within 2%. A benchmark slab phantom test was performed using 6 MV and 10 MV (5 cm × 5 cm field size) x-rays in a solid water/lung/solid water arrangement (Constantinou *et al* 1982, White *et al* 1986) of proportions 4 cm, 8 cm and 4 cm respectively. Farmer chamber (PTW 2333 0.6cc) results were compared with collapsed cone convolution results from Pinnacle 3.

A female ART‡ anthropomorphic phantom was studied for dosimetry within the lung region for a single AP field through heterogeneous lung tissue. CT data for the phantom was attained on a Siemens Somoton plus 4 spiral CT scanner (125 kV, 2 mA) with 2 mm scan thickness. One major factor affecting dosimetry within the ART phantom is the variation in density within the lung area for each phantom slice. The phantom slices are completely covered with approximately 1.5 mm of solid water material at each end. In areas of water equivalent density this does not pose a problem. However, in the lung region where the density ranges
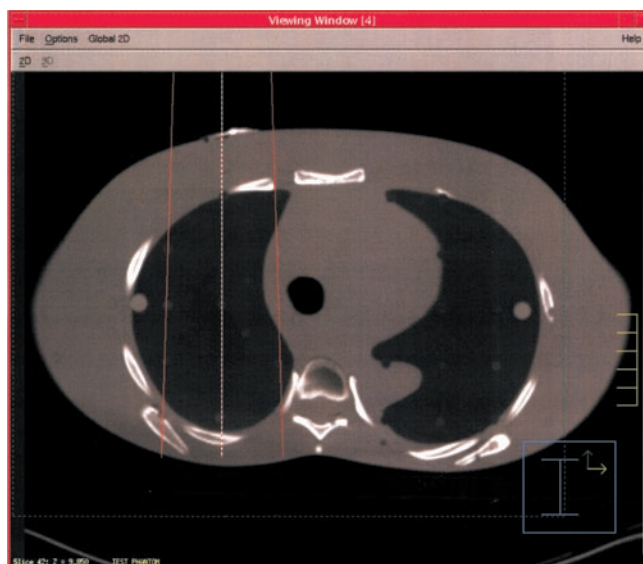
Figure 1. Transverse view of the ART phantom, beam central axis planning slice and field dimension shown for *x* field dimension.

(This figure is in colour only in the electronic version, see www.iop.org)

from 0.3 g cm^{-3} to 0.5 g cm^{-3}, a density of 1 g cm^{-3} covering could produce a distortion in calculated or measured results. Each slice is approximately 2 cm thick, thus the solid water covering (3 mm total from each side accounts for 15% of the target volume). The planning slice is shown in figure 1.

Anthropomorphic measurements were performed using an anterior–posterior (AP) 6 MV field from a Varian 2100C linac. Dosimetry was performed with LiF TLDs and Kodak X-Omat V radiographic film. Lithium fluoride (LiF:Mg:Ti) extruded ribbons were used with a nominal thickness of 0.89 mm. The TLDs were held in tissue equivalent (either muscle or lung, depending on site) cylindrical plugs located at various depths within the phantom. The TL dosimeters were individually calibrated and grouped into sets in which all TL dosimeters shared the same thermal history. In parallel to the *in vivo* measurement, six TLDs from each set were irradiated to a known dose close to the estimated anthropomorphic dose. The unknown anthropomorphic dose was then calculated by using the individual calibration factors of the chips and relating the readings to the readings of the detectors which had received the known dose. This procedure is used to account for daily variations in the TLD reader's photomultiplier collection efficiency. With this procedure, using a NE technology Rialto TLD, uncertainties from fading, thermal treatments and variations of dose response due to radiation quality can be minimized, producing a reproducibility of $\pm 4\%$ (2 standard deviations of the mean) (Kron *et al* 1993). No corrections were applied using Bragg–Gray cavity theory to convert dose absorbed by LiF TLDs to dose in lung, as the effect would be small but present.

The film was positioned in between two phantom slices through the entire phantom. The AP 6 MV field was delivered with an approximately 3° angle to the film to minimize the effects of parallel film exposure (Suchowerska *et al* 1999). The phantom was tightly held together using tape and the screws provided to eliminate as much air gap as possible. The film package was also pierced to eliminate air. For dose calibration, the calibration films were positioned in a solid water phantom of dimensions 30 cm × 30 cm × 30 cm. The phantom
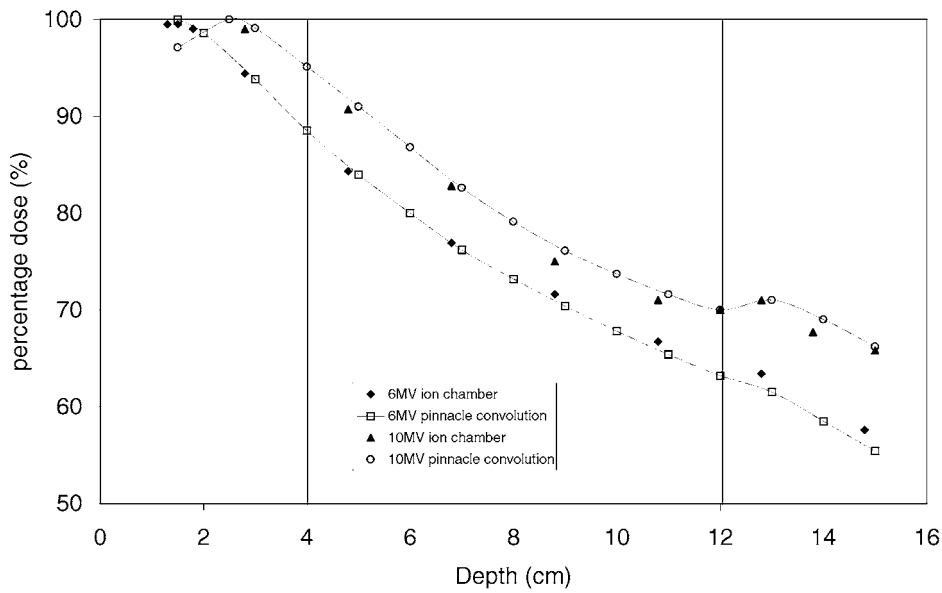
Figure 2. Calculated and measured dose for 6 MV and 10 MV x-ray beams in a solid water/lung/solid water phantom measured with a PTW 2333 0.6 cc ionization chamber (5 cm × 5 cm field and 100 cm SSD).
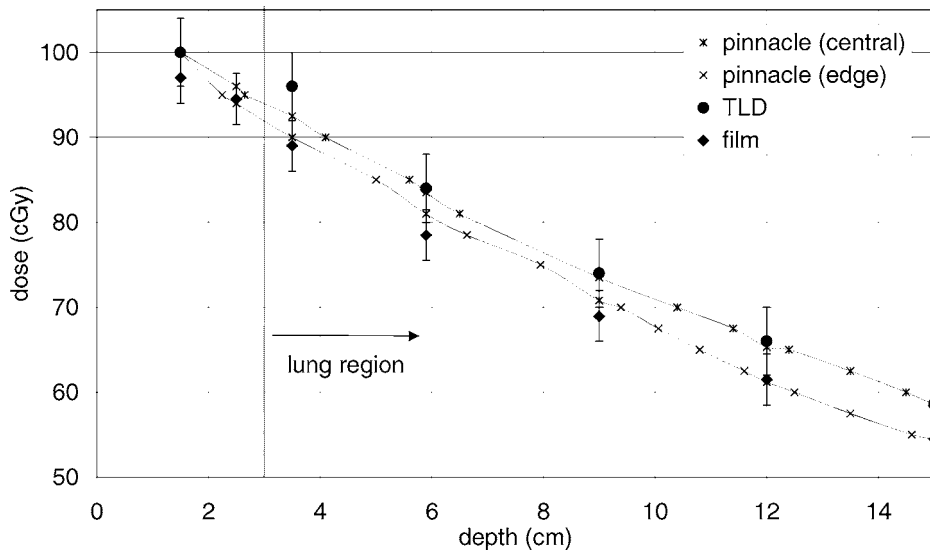

Figure 3. Calculated and measured dose for a 6 MV x-ray beam in a heterogeneous lung phantom. Results are shown for calculated results at the centre of a phantom slice and at the edge of the phantom slice. Radiographic film and TLD results are shown (6 cm × 8 cm field, 100 cm SSD).

was placed on the treatment couch with the upper surface at the isocentre (100 cm). The film was positioned at D_{max}, 1.5 cm for 6 MV x-rays and 2.4 cm for 10 MV x-rays, and doses ranging from 0 cGy to 100 cGy in 10 cGy intervals were given with the film perpendicular to the central axis of the beam. The film was processed in a Kodak M35 X-Omat processor

in a single batch. Film results were analysed with a VIDAR VXR-12 scanner in linear mode and a scanning resolution of 423 microns (Mersseman *et al* 1998). The calibration film's relative density units were then compared to dose by an exponential function. Using the above system a reproducibility of X-Omat V film was found to be $\pm 3\%$ in a homogeneous phantom. Experimental doses were then calculated using the exponential fit derived from the calibration results. Although it is not clear that effective depth is the correct depth for evaluation of film response, a feeling for the magnitude of the film response with depth is needed. Therefore tests were performed to evaluate the sensitivity response of the film at various depths in normal and parallel configurations. For normal film positions, a reduction in sensitivity of 2% was seen from depths of d_{max} to 10 cm. A reduction in sensitivity of 3% for parallel exposed film was seen from the d_{max} position compared to normal exposed film. It is interesting to note that at the depth of d_{max} for a 4 MV x-ray beam, Williamson *et al* (1981) observed approximately 10% under response for parallel exposed films compared to normal films, and Suchowerska *et al* (1999) observed approximately 5–7% over response at 10 cm depth compared to d_{max} in the parallel configuration. Our values were within measured experimental error limits of the film dosimeter; thus no corrections were applied to dose for sensitivity changes in the film associated with spectral changes as the beam was attenuated through the phantom or for film orientation. While the effective depth through the central axis of the planning slice was found to be 6.3 cm water equivalent depth for a physical depth of 18 cm, due to the complexity of interactions between film/lung it is not obvious that either depth would be suitable to apply the depth sensitivity correction. Both film and TLD experiments were repeated five times and the values quoted are the average of these results.

3. Results and discussion

Figure 2 shows the results in the slab phantom. Agreement is good to within 2% for all data points. Collapsed cone convolution accurately calculates a secondary build up at the lung/solid water interface for the 10 MV x-ray beam. The graph shows the collapsed cone calculation giving a slightly higher dose than the ion chamber results in lung at 6 MV and 10 MV just beyond the first tissue–lung interface. This is expected as has been explained by Keall and Hoban (1995, 1996). The overestimation is due to charged particles being more laterally deflected than the kernel density scaling method predicts. Agreement is much better than that previously reported for a scatter function method (effective tissue air ratio) which gave an overestimated mid-lung dose in this phantom for a 5 cm $\times$ 5 cm field of 7.2% (6 MV) and 6.4% (10 MV), while effective depth overestimated the dose by 10.3% (6 MV) and 10.6% (10 MV) (Metcalfe *et al* 1993). While phantom designs vary, there have been several reports showing that corrections based on the scatter function model do not perform accurately for small field sizes where disequilibrium is apparent (Ekstrand and Barnes 1990, Mackie *et al* 1985, Arnfield *et al* 2000).

Figure 3 shows the calculated and measured results for a 6 cm $\times$ 8 cm 6 MV x-ray field incident on the anthropomorphic phantom. Shown are two depth dose curves for dose calculated by collapsed cone convolution at the centre of a 2 cm thick anthropomorphic phantom slice and near the edge of the same phantom slice. This position lies within the solid water coating, approximately 1 mm from the lung, solid water boundary. Differences in calculated dose for these two curves are up to 5% within the lung which was located from 2.5 cm to 15 cm depth. These variations in calculated dose are assumed to be predominantly due to the higher density (1.5 mm solid water) covering of each phantom slice scanned by the CT scanner and reconstructed as a 3D volume in Pinnacle, as is the case for the actual phantom. This coating increases the volume of higher density material which the beam effectively passes through. This is demonstrated by more beam attenuation through the slice edge. TLD experimental results
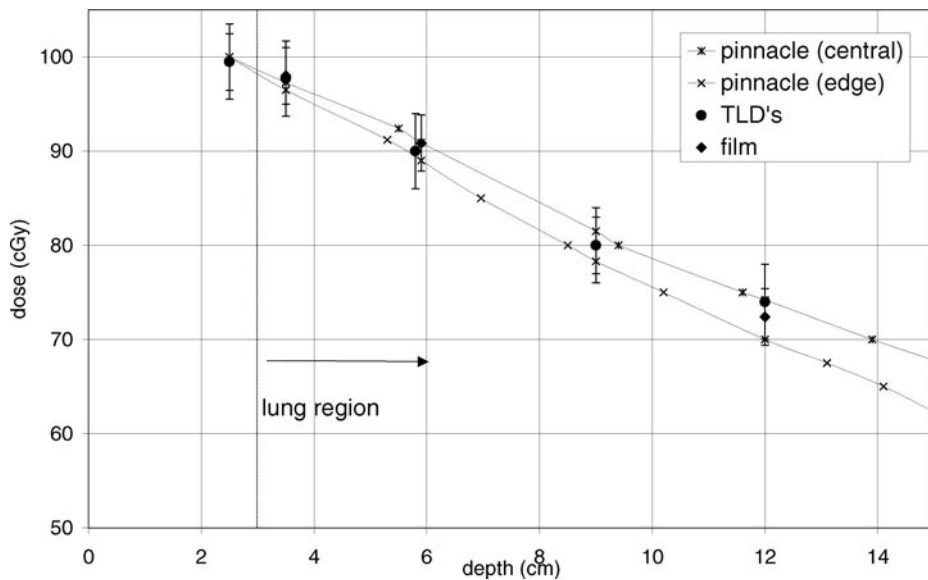
Figure 4. Calculated and measured dose for a 10 MV x-ray beam in a heterogeneous lung phantom. Results are shown for calculated results at the centre of a phantom slice and at the edge of the phantom slice. Radiographic film and TLD results are shown (6 cm × 8 cm field, 100 cm SSD).

match more closely the convolution calculations located at the centre of the phantom slice, which is where the TLDs are physically located during exposure. The film results produced a depth dose curve which matches closer to convolution calculations located at the edge of the phantom, the site of film location. An overestimation of the attenuation caused by the solid water coating of each slice could be expected in the calculation due to the volume generation of the 'solid water' coating slice in the lung region. That is, with a 2 mm slice separation, the planning computer effectively produced a slightly less than 4 mm thick solid water slice in the lung, as opposed to the actual 3 mm solid water slice. Thus Pinnacle effectively grows the width of the high density region by 33% more than reality, though there will be a lessening in the CT density assessment due to a partial volume effect (Metcalfe and Beckham 1988). Thus the overall density assigned is greater than the density of lung. Similar results are seen for 10 MV x-rays, as shown by figure 4. Similar variations for convolution calculation of dose at the centre and edge of the phantom are seen; however, film results are in general slightly higher than the edge calculation, but mostly within error limits. Again the TLD results lie close to the centre calculated dose from Pinnacle.

4. Conclusion

The collapsed cone convolution calculation provides adequate dose accuracy within heterogeneous material in regions of low density such as lung at 6 MV and 10 MV energies. The solid water covering slices of the ART phantom increase the complexity of dose measurement and verification. Both experiment and calculation give similar differences between dose determined at the centre of the slice compared to the dose near the edge of the slice. Verification of the calculation in lung was important as collapsed cone convolution lung plans show differences in dose and isodose coverage when compared to systems using photon scatter based corrections.

References

Ahnesjo A 1989 Collapsed cone convolution of radiant energy for photon dose calculations in heterogeneous media *Med. Phys.* **16** 577–92

Arnfield M, Hartmann Siantar C, Siebers J, Garmon P, Cox L and Mohan R 2000 The impact of electron transport on the accuracy of computed dose *Med. Phys.* **27** 1266–71

Boyer A and Mok E 1986 Calculation of photon dose distributions in an inhomogeneous medium using convolution *Med. Phys.* **13** 503–9

Boyer A and Mok E 1985 A photon dose distribution model employing convolution calculations *Med. Phys.* **12** 169–77

Constantinou C, Attix F and Paliwal B 1982 A solid water phantom material for radiotherapy x-ray and gamma ray beam calibrations *Med. Phys.* **9** 439–41

Ekstrand K and Barnes W 1990 Pitfalls in the use of high energy x-rays to treat tumours in the lung *Int. J. Radiat. Oncol. Biol. Phys.* **18** 249–52

Fraass B, Doppke K, Hunt M, Kutcher G, Starkschall G, Stern R and Van Dyk J 1998 American Association of Physicists in Medicine Radiation Therapy Committee Task Group 53: quality assurance for clinical radiotherapy treatment planning *Med. Phys.* **25** 1773–829

Hoban P W 1995 Accounting for the variation in kerma/terma ratio in photon beam convolution *Med. Phys.* **22** 2035–44

Howlett S, Kron T, Xuan K and Hamilton C 1999 Monitor unit calculations using a 3D computerized treatment planning system: verification in an anthropomorphic phantom *Australas. Phys. Eng. Sci. Med.* **22** 163–5

Keall P and Hoban P 1995 Accounting for primary electron scatter in x-ray beam convolution calculations *Med. Phys.* **22** 1413–18

——1996 Superposition dose calculations incorporating Monte Carlo generated electron track kernels *Med. Phys.* **23** 479–86

Kron T *et al* 1993 X-ray surface dose measurements using TLD extrapolation *Med. Phys.* **20** 703–11

Mackie T, Bielajew A, Rogers D and Batttista J 1988 Generation of photon energy deposition kernels using the GES Monte Carlo system *Phys. Med. Biol.* **33** 1–20

Mackie T, El-Khatib E, Battista J, Scrimger J, Van Dyk J and Cunningham J 1985a Lung dose corrections for 6 and 15 MV x-rays *Med. Phys.* **12** 327–32

Mackie T, Scrimiger J and Battista J 1985b A convolution method of calculating dose for 15 MV x-rays *Med. Phys.* **12** 188–96

Mersseman B and De Wagter C 1998 Characteristics of a commercially available film digitizer and their significance for film dosimetry *Phys. Med. Biol.* **43** 1803–12

Metcalfe P, Wong T and Hoban P 1993 Radiotherapy x-ray beam inhomogeneity corrections: the problem of lateral electronic disequilibrium in lung *Australas. Phys. Eng. Sci. Med.* **16** 155–67

Metcalfe P and Beckham W 1988 Radiotherapy planning accuracy in terms of CT numbers and inhomogeneity correction techniques *Aust. Radiol.* 371–79

Mohan R, Chui C and Lidofsky L 1986 Differential pencil beam dose computation model for photons *Med. Phys.* **13** 64–73

Papanikolaou N, Mackie T, Meger-Well C, Gehring M and Reckwerdt P 1993 Investigation of the convolution method for polyenergetic spectra *Med. Phys.* **20** 1327–36

Ramsey C R, Cordrey I L, Spencer K M and Oliver A L 1999 Dosimetric verification of two commercially available three-dimensional treatment planning systems using the TG-23 test package *Med. Phys.* **26** 1188–95

Suchowerska N, Hoban P, Davison A and Metcalfe P 1999 Perturbation of radiotherapy beams by radiographic film: measurements and Monte Carlo simulations *Phys. Med. Biol.* **44** 1755–65

Van Dyk J, Barnett R B, Cygler J E and Shragge P C 1993 Commissioning and quality assurance of treatment planning computers *Int. J. Radiat. Oncol. Biol. Phys.* **20** 261–73

White D R, Constanitinou C and Martin R 1986 Foamed epoxy resin-based lung substitutes *Br. J. Radiol.* **59** 787–90

Williamson J F, Khan F M and Sharma S C 1981 Film dosimetry of megavoltage photon beams: a practical method of isodensity-to-isodose curve conversion *Med. Phys.* **8** 94–8